Talanta 120 (2014) 283–288

Contents lists available at ScienceDirect

Talanta

journal homepage: www.elsevier.com/locate/talanta

Data handling of GC/MS signals for characterization of PAH sources in Northern Italy aerosols

M.C. Pietrogrande [a,*], M.G. Perrone [b], G. Sangiorgi [b], L. Ferrero [b], E. Bolzacchini [b]

[a] Department of Chemical and Pharmaceutical Sciences, University of Ferrara, Via Fossato di Mortara, 17, 44100 Ferrara, Italy
[b] Department of Earth and Environmental Sciences, University of Milano-Bicocca, P.zza della Scienza 1, 20126 Milan, Italy

ARTICLE INFO

Article history:
Received 14 August 2013
Received in revised form
28 November 2013
Accepted 4 December 2013
Available online 16 December 2013

Keywords:
Polycyclic aromatic hydrocarbons
GC/MS signal processing
Source profiles
Data handling

ABSTRACT

The paper describes the characterization of polycyclic aromatic hydrocarbons (PAHs) in atmospheric aerosol samples using Gas Chromatography–Mass Spectrometry analysis. A data handling of GC/MS signals based on Experimental Autocovariance Function (EACVF) is described in order to directly characterize PAHs with a simple and reliable method suitable for processing large batches of samples.

The method was successfully applied to 42 aerosol samples collected in different seasons (summer, fall and winter) in two locations in Northern Italy: Milan, a large urban area, and Oasi Le Bine, a rural site. The reliability of the EACVF results was verified by comparison with the values computed with the conventional GC/MS signal treatment and the data of independent studies.

Two main emission sources were identified and described by PAH concentration profiles: the road traffic source (TR), characterized by high contributions of FLNT, PYR and CHR, and the residential combustion (COMB) mainly containing pyrogenic high molecular weight PAHs, i.e., CHR, BaP, BeP, BbF and BkF. In addition, some PAH diagnostic ratios were directly computed for the EACVF plot, to distinguish between traffic and combustion dominated emissions, i.e. the ratios CHR/BaP, PYR/BaP and PYR/BeP.

1. Introduction

In environmental monitoring and assessment studies there is an increasing concern about identification and quantification of chemical markers to adequately represent a chemical signature of the possible organic source inputs to atmospheric particle matter (PM). Among them, polycyclic aromatic hydrocarbons (PAHs) have been recognized especially suited to trace the origin and fate of different PM samples because they are produced by multiple sources involving combustion, since they are formed primarily during the incomplete combustion of fossil fuels (petroleum, natural gas and coal) and biomass burning [1–10]. PAH distribution profiles in PM emissions from various sources are becoming more widely used for evaluating the chemical composition and emission strength of particulate emissions [6,10–14]. As a consequence of the growing concern over concentration levels of PAHs in ambient air, optimization of the analytical methods is needed on the basis of simplicity and efficiency, in order to process large batches of samples.

Gas chromatography coupled with mass spectrometry (GC/MS) is the well-established technique of choice for identifying and quantifying PAHs in complex mixtures of organics such as those present in aerosol samples [1–9]. The GC/MS signal obtained is usually a complex chromatogram, containing many resolved and unresolved peaks; for this reason, it is difficult to extract all the analytical information hidden in the chromatogram and hence the resulting estimate may be unreliable. Moreover, the conventional method for chromatogram data processing requires subsequent steps, including identification, by comparison with reference standards and MS spectra, quantification of individual PAHs and computation of their diagnostic parameters.

Therefore, signal processing procedures are very helpful in transforming the GC data into usable chemical information: in particular, a computer-assisted method has to be preferred as a high-throughput approach since it reduces the labor and time required to handle the extensive amounts of data produced by environmental monitoring. Among the many signal processing procedures developed to deal with this problem, an approach based on the Autocovariance Function (ACVF) has been developed

Abbreviations: ACVF, Autocovariance Function; COMB%, relative abundance of PAHs from combustion sources computed with the traditional procedure; $COMB\%_{EACF}$, COMB% computed with the EACVF method; Δt, correlation time between the positions of the digitized chromatogram on which EACVF is computed; EACVF, experimental autocovariance function computed on the total chromatogram; GC/MS, gas chromatography coupled with mass spectrometry; PAHs, polycyclic aromatic hydrocarbons; PM, particle matter; TR%, relative abundance of PAHs from traffic sources computed with the traditional procedure; $TR\%_{EACVF}$, TR% computed with the EACVF method

* Corresponding author. Tel.: +39 05 32 45 5152.
E-mail address: mpc@unife.it (M.C. Pietrogrande).

0039-9140/$ - see front matter © 2013 Elsevier B.V. All rights reserved.
http://dx.doi.org/10.1016/j.talanta.2013.12.010

and widely applied to experimental chromatograms [15–20]. Recently, the approach has been applied for tracking the biogenic and anthropogenic origins of n-alkanes in PM samples [21].

This study was designed as a further application of the ACVF approach to handle GC/MS signals of PM samples in order to develop and validate the method for characterizing PAH abundances and distribution to be related to source profiling. Thanks to the method, main information on PAHs—the relative contribution of major sources, like traffic and domestic heating, to the total PAH content and some diagnostic ratio values—can be directly estimated from the chromatogram and the PC computation takes just a few seconds.

1.1. GC/MS signal processing procedure based on Autocovariance function

An approach based on the AutoCovariance Function has been developed to interpret the complex GC/MS signals. ACVF can be directly computed from the original chromatogram experimentally acquired in digitized form (Experimental ACVF, EACVF) using the following expression [18]:

$$\mathrm{EACVF}(\Delta t) = \frac{1}{N}\sum_{j=1}^{N-k}(Y_j - \hat{Y})(Y_{j+k} - \hat{Y}) \quad k = 0, 1, 2, \ldots M-1 \tag{1}$$

where Y_j is the digitized chromatogram signal at the acquisition point j, N the number of points of the digitized chromatogram, M the truncation point in the EACVF computation. The correlation time Δt is the interdistance between the positions of the digitized chromatogram: it assumes discrete values $\Delta t = k\tau$, with k ranging from 0 to $(M-1)$, where τ is the time interval between the subsequent acquisition points of the digitized signal.

To increase the method reliability in comparing different signals, a normalization approach is applied by computing the Autocorrelation Function EACF(Δt) as a relative value referred to EACVF(0), which is the EACVF(Δt) value at $\Delta t = 0$

$$\mathrm{EACF}(\Delta t) = \frac{\mathrm{EACVF}(\Delta t)}{\mathrm{EACVF}(0)} \tag{2}$$

EACF(Δt) can be plotted vs. the interdistance Δt to obtain the EACF plot. As an example, Fig. 1a reports the EACF(Δt) plot computed on the GC/MS signal reported in the figure detail: it represents a $PM_{2.5}$ sample collected in the urban site MI in summer (bold line in the EACF plot).

In essence, the method consists in singling out the correlations among peak positions in the complex chromatographic signal. In fact, peak signals randomly distributed in the complex chromatogram generate EACF values close to 0, while peaks placed at ordered interdistances Δt (signed by arrows in the chromatogram of Fig. 1a) produce well-defined Gaussian peaks located at Δt values in the EACF plot (circles in the figure). Such ordered structures (representing the Deterministic component of the signal) correspond to the most abundant peaks or peaks located at constant interdistances repeated in the chromatogram [18]. The result is that the EACF plot is a simplified picture of the original chromatographic profile, which singles out the main information on the separation pattern related to the chemical composition of the analyzed sample. The consequent high simplicity of the EACF plot allows us to easily single out regularities in the retention pattern so that it may be proposed as a simplified fingerprint of the chromatographic profile to characterize and compare complex samples.

In addition, the EACF plot also contains information on quantitative composition of the sample, since the height of each EACF peak is related to the abundance of the repetitiveness in the chromatogram, i.e., the combination of the number of repeated peaks and their heights.

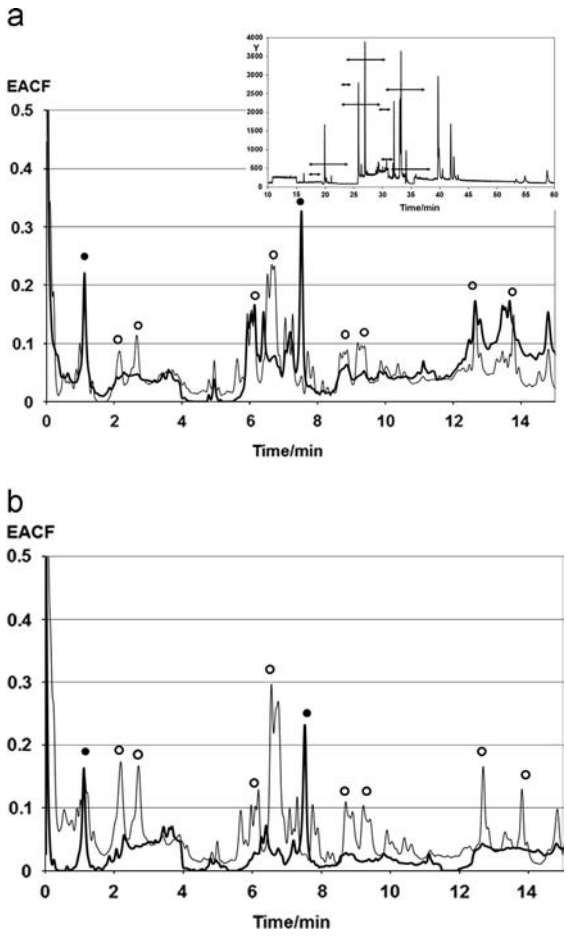

Fig. 1. EACF plots computed on the GC/MS chromatograms of PM samples. The circles indicate the deterministic EACF peaks generated by PAHs from traffic emissions (TR%, full circles) and combustion sources (COMB%, open circles). (a) EACF plots of the PM samples collected in the urban site in winter (plain line, sample MI_win_$PM_{2.5}$_4) and in summer (bold line, sample MI_sum_$PM_{2.5}$_2). Figure inset: GC/MS signal of MI_sum_$PM_{2.5}$_2 sample used to compute EACF plot; arrows: interdistance values generating the deterministic EACF peaks. (b) EACF plots of the PM samples collected in the rural site in winter (plain line, sample OB_win_$PM_{2.5}$_1) and in summer (bold line, sample OB_sum_$PM_{2.5}$_2).

In particular, a simplified model has been implemented able to estimate the relative contribution of a deterministic component (with total area A_D) directly from the EACF(Δt) values, according to the following equation:

$$\mathrm{EACF}(\Delta t) = \frac{\mathrm{EACVF}(\Delta t)}{\mathrm{EACVF}(0)} \approx \frac{A_D^2\, m_{tot}}{m_D\, A_T^2} \approx \frac{A_D}{A_T} \tag{3}$$

The detailed description of the mathematical equations used in developing the simplified model is reported in the Supplementary information (SI). Using Eq. (3) the following information on PAHs can be directly estimated from the EACF(Δt) values:

- the contribution of a selected group of PAHs (with total area A_D) to the whole area of the chromatogram (A_T);
- the ratio between the area of specific PAHs by properly selecting EACF(Δt) values computed at Δt corresponding to the selected PAHs.

It must be underlined that this statistical approach includes normalization since the EACF values are related to EACVF(0) values referring to the total chromatographic signal: this procedure reduces the anomalies in peak integration and guarantees more accurate

results in PAH signatures in comparison with un-normalized signatures [18,21].

In summary, the EACF method displays three fundamental advantages, in comparison with the traditional procedure based on computation performed on integrated area of PAH peaks:

- it saves time and labor in data handling, thus increasing throughput and flexibility;
- it reduces the subjectivity of human intervention, thus improving data quality;
- it increases result reliability by singling out the contribution of selected peaks.

2. Materials and methods

2.1. Sample collection

The approach used for PM sampling, as well as the description of sampling sites and of seasonal sampling campaigns, is reporeted in detail in our previuous papers [22,23]. Briefly, the PM samples were collected at two locations in Northern Italy: at an urban (MI) and a rural site (OB). The Milan site (MI; 45°31′19″N, 9°12′46″E) is located at "Torre Sarca", close to the University of Milano-Bicocca, and is representative of high vehicle traffic conditions. The Oasi Le Bine site (OB; 45°08′40″N, 10°26′08″E) is located far from any big city centers, the nearest cities of Cremona and Mantova are about 15–20 km away: it represents a rural environment. PM sample collection was during summer (July–Agust 2008), fall (November 2008) and winter (December 2008–January 2009) at both sites.

PM samples were daily (24 h) collected using low-volume gravimetric samplers (flow 38.33 l/min: HYDRA sampler, FAI Instruments, Rome, Italy) on Quartz-fiber filters (Ø=47 mm, Whatman, USA; prebaked at 600 °C for 2 h). Before and after sampling, filters were equilibrated (48 h at 35% RH, ambient T) and weighted with a microbalance (1 μg precision, model M5P-000V001 Sartorius, Germany) in order to measure particle concentration (μg m^{-3}).

All sampled filters were then kept in the dark at −20 °C (to avoid photo-degradation and evaporation) for the purpose of chemical analysis. A total of 42 PM samples were analyzed in the present study: samples were categorized according to the sampling site (MI, OB), seasonality (winter, fall and summer) and particle size (PM_{10}, $PM_{2.5}$ and PM_1) (Table S1 in Supplementary information).

2.2. Sample preparation

For PAHs analysis, PM filters were extracted in 2 ml of dichloromethane: (CH_2Cl_2, purity ≥ 99.8%, Ultra Resi-Analyzed, J.T. Baker) for 20 min in an ultrasonic bath (Sonica®, Soltec, Italy). The extract was then filtered through a PTFE syringe filter (cut 0.45 μm, Alltech, USA) to remove insoluble particles. The extraction solvent was evaporated under a gentle stream of nitrogen (N_2, purity ≥ 99.9999%, Sapio, Italy) until dryness. The residue was dissolved in 200 μl of isooctane (C_8H_8, purity ≥ 99.5%, for residue analysis, Fluka), and analyzed within 24 h from extraction.

2.3. GC/MS analysis

The isooctane extract was analyzed for PAHs by Gas Chromatography coupled with Mass Spectrometry. An Agilent 6850 GC was used, equipped with an autosampler and a split/splitless injector. The separation was performed on a DB-XLB capillary column (length 60 m, i.d. 250 μm, film 0.25 μm; J&W Scientific). The injector was kept at 280 °C and 2 μl of extract were injected in splitless mode. Helium (He; purity 99.999%, Sapio, Italy) was used as carrier gas with a constant flow of 1 mL min^{-1}. The temperature program for PAHs analysis was: from 80 °C to 150 °C at 40 °C min^{-1}, from 150 °C to 300 °C at 5 °C min^{-1}, isothermal hold at 300 °C for 30 min, and from 300 °C to 330 °C at 40 °C min^{-1} with isothermal hold at 330 °C for 16 min. The transfer line was kept at 310 °C.

A quadrupole mass spectrometer (5973 Network Mass Selective Detector, Agilent Technologies) was used and operated at 70 eV in the electron ionization (EI) mode. The chromatograms were acquired in the SIM (Single Ion Monitoring) mode: m/z values corresponding to the molecular weight of each PAH were used for quantification. GC/MS data of the PAHs analyzed are reported in the Supplementary information (Table S2, containing elution time and diagnostic ions of each analyte).

Twenty PAHs were determined: naphthalene (NAPH), acenaphtylene (ACTY), acenaphtene (ACT), fluorene (FLN), phenanthrene (PHE), anthracene (ANT), fluoranthene (FLNT), pyrene (PYR), benzo[a]anthracene (BaA), cyclopenta[cd]pyrene (CPcdP), chrysene (CHR), benzo[b]fluoranthene+benzo[j]fluoranthene (BbF+BjF), benzo[k]fluoranthene (BkF), benzo[e]pyrene (BeP), benzo[a]pyrene (BaP), dibenzo[a,h]antracene (dBahA), indeno[1,2,3–cd]pyrene (IcdP), benzo[ghi]perylene (BghiP), dibenzo[a,e]pirene (dBaeP). We note that BbF and BjF coeluted, and thus they were determined together (BbF+BjF).

The PAHs were identified by matching the retention times of each peak in the sample chromatogram with those of a standard solution. Interfering coelution problems were evaluated in the samples by comparing mass spectra of the samples with those of the standards as well as with those from the NIST mass spectra library (NIST MS Search r. 2.0).

The external standard method was used for PAH quantification. Daily calibration curves were obtained from standard mixtures of PAHs (10 μg ml^{-1} of each PAH) and showed good linearity with regression coefficients $R^2 > 0.995$ for all PAHs. Analytical repeatability was assessed in the 5–20% range. The reference standard SRM1649a (Standard Urban Dust Reference Material, NIST, USA) was used to evaluate extraction efficiency for PAHs from PM samples. The estimated % of recovery were > 70% for the analyzed PAHs, with the exception of the most volatile PAHs, NAPH, ACTY and ACT, for which 10–30% values were found.

2.4. Computations on GC/MS signals

All the programs are written in Fortran and run on a 2 GHz (512 RAM), Pentium III personal computer. EACVF(Δt) was numerically calculated from the digitized chromatogram, according to Eqs. (1 and 2), and the PAH parameters were directly estimated from EACVF(Δt).

3. Results

3.1. Data handling of GC/MS signals using the EACF method

The EACF method was applied to the GC/MS signals of 42 PM samples varying in the sampling site, urban (MI) and rural (OB), seasonality (winter, fall and summer) and cutpoint inlets used for collection (2.5 μm and 1 μm in all the sampling sites and 10 μm cutpoint in MI). A complete list of the studied samples is reported in Table S1 in Supplementary information.

The EACF was directly computed on the GC/MS signal (SIM signal at m/z values reported in Table S1): the region 8–75 min was selected, since it contains all the twenty PAHs analyzed. The obtained results are summarized in Table 1 (data of the samples reported in Fig. 1 and mean values averaged according to sampling site and seasonality) and extensively reported for all the investigated samples in Table S1 in Supplementary information.

Table 1
PAH parameters computed in the investigated PM samples with the traditional procedure (1st, 3rd, 5th, 7th and 9th columns) and the EACVF method (2nd, 4th, 6th, 8th and 10th columns). The reported parameters are: TR% and COMB% (the relative contribution of the traffic and combusution emission sources related to the total PAH amount) and the PAH diagnostic ratios CHR/BaP, PYR/BeP and PYR/BaP. The reported values describe the PM samples investigated with the EACF plots reported in Fig. 1. Mean values are computed on the PM samples collected in MI and OB sites in the same season.

	TR%	TR% *EACVF*	COMB%	COMB% *EACVF*	CHR/BaP	CHR/BaP *EACVF*	PYR/BaP	PYR/BaP *EACVF*	PYR/BeP	PYR/BeP *EACVF*
MI_win_$PM_{2.5}$_4	35	39	53	52	1.7	1.1	1.8	0.9	2.3	2.2
MI_win_mean	33	34	58	65	1.7	1.3	1.3	1.0	1.7	2.1
MI_fa_mean	28	28	57	61	1.1	0.7	1.0	0.7	1.2	1.5
MI_sum_$PM_{2.5}$_2	47	47	14	14	1.9	1.8	2.6	1.7	4.3	4.7
MI_sum_mean	43	45	21	20	2.8	2.5	4.3	4.3	4.7	4.8
OB_win_$PM_{2.5}$_1	24	24	67	67	1.3	1.0	0.8	0.6	0.7	1.3
OB_win_mean	23	23	66	71	1.3	1.0	0.8	0.4	0.7	1.2
OB_fa_mean	22	22	64	70	1.0	0.6	0.7	0.7	0.9	1.8
OB_sum_$PM_{2.5}$_2	46	46	10	10	1.5	1.2	9.0	9.4	17	18
OB_sum_mean	52	52	11	11	1.5	1.3	10	10	16	17

In general, the EACF plots (Fig. 1a,b) show a common feature for all the PM samples collected in the same sampling site, Milan vs. Oasi Le Bine, in the same season. Winter and fall samples show close features recognized by several deterministic peaks, as shown by the plain lines in Fig. 1a,b which report the EACF plots computed on $PM_{2.5}$ filters sampled in Milan (MI, Fig. 1a, 1st row in Table 1) and in the rural site (Fig. 1b, 6th row in Table 1). Samples collected in the hot season generate EACF plots characterized by a simplified pattern, as shown by the bold lines in Fig. 1a,b for the filters sampled in Milan (Fig. 1a, 4th row in Table 1) and in the rural site (Fig. 1b, 9th row in Table 1).

By comparing the obtained EACF plots with those obtained from GC/MS analysis of PAH standard mixtures, it is possible to identify the specific PAHs which mainly contribute to the highest deterministic peaks, i.e., the most abundant PAHs or those displaying the most repeated peak interdistances. The deterministic peaks at $\Delta t = 1.1$ and 7.4 min are mainly produced by the high peaks of FLNT, PYR and CHR, those at $\Delta t = 6$ and 13.4 min are mostly due to the contribution of CHR and BaA. The other peaks at $\Delta t = 2.1$, 2.6, 6.5, 8.5, 9.2 and 12.5 min are generated by the combination of signals of pyrogenic high molecular weight PAHs: CHR, BaP, BeP, BbF+BjF and BkF.

3.2. Identification of PAH source profiles

Several studies have been performed to characterize PAH profiles in PM emissions from various sources, i.e., road traffic emissions, including gasoline-powered and diesel-powered vehicles, residential heating, including wood and coal combustion and natural gas-fired home appliance or their mix, biomass burning and industrial processes [6,10–14]. However, this approach is limited by the difficulty in the chemical characterization of PM samples due to complexity of the chromatographic signal and low reproducibility of chromatographic instruments and experimental conditions.

Here, the EACF plot is proposed as a simplified fingerprint of structure and abundance of PAHs present in the sample to describe PAH source profiles. The information extracted from EACF plots were related to known source profiles of airborne PAHs. Traffic and biomass burning have been identified by several studies as the major emission sources for PAHs in Northern Italy [22–28].

Concerning the contribution of traffic source, the chemical profiles of emissions from gasoline-powered and diesel-powered vehicles have been found largely influenced by several factors, including different fleet compositions, driving patterns, climate conditions and fuel compositions [11–13]. In the present study a traffic source profile derived from a roadside tunnel study performed in Milan was used to closely reflect actual fleets of on-road vehicles [22]. Traffic source of PAHs in Milan has been found dominated by emissions from diesel vehicles that contribute nearly 10 times more than gasoline vehicles [27]. The traffic profile in Milan, with a prevailing diesel contribution, is characterized by high amount of lighter PAHs, such as PHE, FLNT, and PYR, and this typical traffic profile for PAHs is characteristic for other EU countries too, where the contribution of diesel vehicles is relevant, as also reported by El Haddad for a tunnel study in France [13].

The GC/MS signal of PHE, FLNT, and PYR produces the EACF deterministic peaks at $\Delta t = 1.1$ and 7.4 min that are then proposed to visualize traffic profile (TR, indicated by full circles in Fig. 1). The relative contribution of traffic source to total PAHs (TR%) can be quantified by the ratio between the abundances of the three compounds ($\sum$TR = FLNT + PHE + PYR) and $\sum$PAHs.

Concerning combustion sources, data from recent monitoring results and emissions inventories showed that PAH emission from residential heating in the Lombardy Region is strongly impacted by the contribution of biomass burning, mainly traditional wood stoves, closed fireplaces and open fireplaces [22,24,25,27,28]. Several studies suggest that such emissions are predominantly characterized by pyrogenic high molecular weight PAHs: CHR, BaA, BaP, BeP, BbF+BjF, BkF. The EACF plot computed on the GC/MS signal of these PAHs is characterized by deterministic peaks at $\Delta t = 2.1$, 2.6, 6, 6.5, 8.5, 9.2, 12.5 and 13.4 min. Therefore such peaks are proposed to describe combustion profile (COMB, indicated by open circles in Fig. 1). Usually the combustion contribution (COMB%) may be quantified by the ratio between the sum of typically pyrogenic PAHs ($\sum$COMB = CHR + BaA + BbF + BjF + BkF + BaP + BeP) and $\sum$PAH [1,4,14].

Therefore the TR% and COMB% values can be directly computed from the EACF obtained from the GC/MS signal by skipping steps of the traditional procedure, requiring just a few seconds of PC computation time (algoritm based on Eq. (3)). More simply, a visual inspection of the EACF plots (Fig. 1) shows the relative contribution of the different sources: the deterministic peaks at $\Delta t = 1.1$ and 7.4 min are diagnostic of traffic emission (full circles) while the peaks at $\Delta t = 2.1$, 2.6, 6, 6.5, 8.5, 9.2, 12.5 and 13.4 min indicate the contribution of combustion profile (open circles). In the rural site the PAH profiles are clearly dominated by vehicle emissions in summer and combustion in winter (Fig. 1b, bold and plain lines, respectively). In Milan airborne PAHs are produced by a combination of the two sources with higher contribution of traffic in summer and of combustion in winter (Fig. 1a, bold and plain lines, respectively).

3.3. Estimation of PAH sources

To test the reliability of the EACF results, all the investigated PM samples were submitted to the traditional procedure on the GC/MS chromatograms (1st and 3rd columns in Tables 1 and S1) or to EACF computations (2nd and 4th columns) to evaluate the

relative contributions of the two main sources, TR% and COMB%. The two series of obtained data were compared by computing the correlation relationships: the good correlation coefficients and the slope values close to 1 (1st and 2nd rows in Table 2) are an experimental proof of the reliability of the EACF procedure in investigating PAH profiles.

In general, the obtained data show very similar parameters for the three particulate sizes investigated: in fact nearly identical TR% and COMB% values were observed in PM_1, $PM_{2.5}$ and PM_{10} samples collected from the same site, on the same days. This is consistent with the results of various authors that found that the PAH emission is mainly associated with the fine and ultrafine particles, in particular, the PAHs with four or more structural rings are concentrated in $PM_{0.2-2.5}$ fractions [29–31]. As a consequence, both $PM_{2.5}$ and the PM_{10} samples are equally useful for PAH investigations, such as speciation and source apportionment studies.

By combining the parameters TR% and COMB%, computed with both the procedures, total values close to 80% (average 80% ± 9%) were obtained for all the analyzed samples, independently of sampling site and seasonality. These results suggest that nearly 20% of the investigated PAHs are not apportioned by the two main sources identified and may be produced from unidentified sources (e.g., industrial source) as well it may be due to PAHs reactivity [9,10].

To investigate spatial and temporal characteristics and source contributions to PAHs the parameter COMB% derived from EACF was plotted as a function of TR% for each PM sample (plot reported in Fig. 2). The main PM classification is based on seasonal differences, with fall and winter data showing very similar behaviors, and is less accounted for the sampling site.

Such discrimination is due to predominant emissions from combustion source of PAHs (mainly burning of biomass for residential heating) during winter and fall (COMB% mean values = 66% and 67%, respectively). In summer the dominating contributor of PAHs is vehicular emission (TR% mean value = 45%).

In addition to this classification, a significant variation in the two sampling sites can be identified: in the cold seasons, the rural site OB is characterized by lower traffic contribution (TR% = 17–24%)—and accordingly higher combustion contribution (COMB% = 58–84%)—in comparison with the urban location (TR% = 20–42%, COMB% = 49–71%) revealing a lower contribution from vehicle emissions.

These results are in agreement with the source contribution to ambient PAHs concentration estimated by Chemical Mass Balance (CMB) modeling at the sites of MI and OB [22]. CMB results indicated that PAHs derived almost completely ($\geq$75%) from biomass burning at the rural OB site; instead the TR source accounted more than 50% of PAHs at the urban MI site in summer (but less than 20% in winter). These findings are also consistent with the emission inventory in Lombardy region that identifyied biomass burning as the major source of BaP, responsible of 78% of total emissions on yearly basis [27]. Similar results have been reported for different cities, where high proportion of the PAH ambient air concentration in fall and winter is associated with the predominant contribution of coal, wood, and peat burning [7].

Table 2
Statistical parameters for the correlations between PAH parameters computed with the traditional and the EACVF procedures.

Parameters	b_1	b_0	R^2
TR%	0.96 ± 0.04	2.1 ± 0.5	0.973
COMB%	0.96 ± 0.04	2.0 ± 0.3	0.974
CHR/BaP	0.99 ± 0.04	0.30 ± 0.08	0.951
PYR/BaP	1.11 ± 0.03	0.4 ± 0.1	0.965
PYR/BeP	0.95 ± 0.04	0.6 ± 0.1	0.980

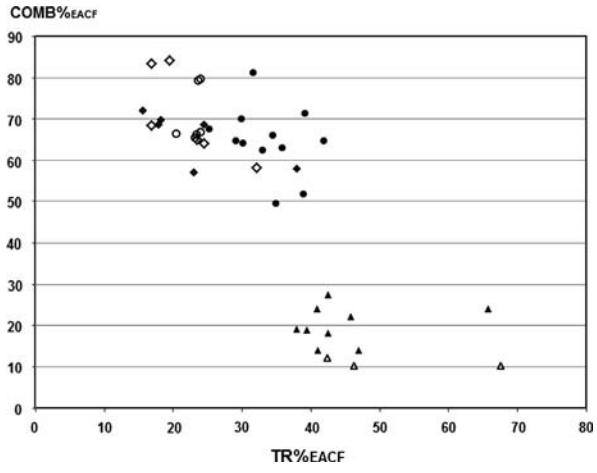

Fig. 2. Characterization and classification of the different PM samples based on the parmeters computed by EACF: relative contribution of traffic emissions (TR%) and combustion sources (COMB%). Symbols identify the the seasonality (circles: winter; squares: fall; triangles: summer) and colors the sampling sites (full: Milan; open: Oasi le Bine).

3.4. Computation of PAH diagnostic ratios

In addition to the comprehensive description of the chromatographic finger print, the EACF approach is here proposed to extract information on the abundance of those specific PAH tracers which are frequently used to compute diagnostic binary ratios for source identification [1,10,32]. Though the ratio method requires caution to avoid wrong discrimination between some sources, it can help in the assessment of the prevailing PAH source and can be improved by using various ratios simultaneosly and performing their relative comparison. This study is focused on the PAH ratios useful to distinguish between traffic and combustion dominated PAH profiles, i.e. CHR/BaP, PYR/BaP and PYR/BeP. The EACF deterministic peaks that are mainly produced by specific PAHs can be identified by comparison with the GC/MS signals of PAH standard mixtures.

The CHR peak mainly produces the EACF deterministic peaks at Δt = 1.1 and 7.4 min, PYR those at a Δt = 6 and 13.4 min, BaP those at Δt = 2.1, 2.6 and 12.5 min, and finally BeP the EACF peaks at Δt = 8.5 and 13.4 min. Therefore the ratios CHR/BaP, PYR/BeP and PYR/BaP can be directly evaluated from the EACF(Δt) values related to the areas of the corresponding peaks (Eq. (3)) (6th, 8th and 10th columns). For comparison, the diagnostic ratios were computed for all the 42 investigated PM samples by using the traditional procedure (5th, 7th and 9th columns in Tables 1 and S1). The correlation between the two data sets was evaluated: the goodness of the regression fits characterized by correlation coefficients and slopes close to 1 (0.95 – 0.98 and 0.95 – 1.1, respectively) indicates that the EACF procedure provides an accurate estimation of the PAH ratios (3rd–5th rows in Table 2).

The CHR/BaP ratio can be used to distinguish between traffic and combustion dominated PAH profiles: in fact PAHs resulting from the use of coal, oil, and wood are low in CHR relative to BaP in comparison with mobile source combustion emissions from diesel and petroleum [1,33]. In our case, the ratio values were higher in summer (mean values: 1.8 and 1.2 and for MI and OB sites, respectively) in comparison with winter and fall (mean values: 1.0 and 0.8 for MI and OB sites, respectively) confirming the lowest contribution of combustion emissions in the hot season, in particular in the urban site.

These results can also be confirmed by the binary ratio PYR/BaP, since mobile source combustion emissions were found high in PYR relative to BaP yielding higher ratios than those of residential

combustion emissions. The values obtained in summer (mean values: 4.3 and 10 in Mi and OB sites, respectively) make it possible to diagnose the predominant contribution of the traffic emission in comparison with the lower contribution in the cold seasons, characterized by lower ratios, i.e., winter and fall mean values: 0.8 and 0.6 in Mi and OB sites, respectively.

Finally, similar information can be obtained from the PYR/BeP, since high values are diagnostic of PAH traffic contribution: values higher than 6 have been found for highway tunnels heavily exposed to auto-mobile exhaust gases from diesel and gasoline cars [11–13,33]. In our study the high values found in summer samples (mean values: 4.8 and 17 in Mi and OB sites, respectively) indicate a strong contribution of vehicle emissions, while the results found in cold seasons (winter and fall mean values: 1.8 and 1.5 in Mi and OB sites, respectively) are consistent with a combined contribution from combustion emissions.

4. Conclusions

Our results provide experimental evidence of the usefulness of the EACF procedure for simple, quick characterization of PAH source profiles in PM samples as a reliable alternative to the traditional procedure based on chromatogram integration. This approach overcomes the difficulty in the chemical characterization of PM samples due to complexity of the chromatographic signal and low reproducibility of chromatographic instruments and experimental conditions and increases GC/MS analysis throughput and flexibility without sacrificing data quality or reliability of the results. This property is especially helpful for characterizing the distribution patterns of PAHs as chemical tracers in organics input sources to be used whenever attempting to identify the origin of an aerosol for the purpose of pollution control or abatement.

Appendix. Supplementary information

Supplementary data associated with this article can be found in the online version at http://dx.doi.org/10.1016/j.talanta.2013.12.010.

References

[1] K. Ravindra, R. Sokhi, R. Van Grieken, Atmos. Environ. 42 (2008) 2895–2921.
[2] X. Bi, B.R.T. Simoneit, G. Sheng, S. Ma, J. Fu, Atmos. Res. 88 (2008) 256–265.
[3] B. Van Drooge, P.P. Ballesta, Environ. Pollut. 158 (2010) 2880–2887.
[4] M.C. Pietrogrande, G. Abbaszade, J. Schnelle-Kreis, D. Bacco, M. Mercuriali, R. Zimmermann, Environ. Pollut. 159 (2011) 1861–1868.
[5] J. Schauer, G.R. Cass, Environ. Sci. Technol. 34 (2000) 1821–1832.
[6] A.L. Robinson, R. Subramanian, N.M. Donahue, A. Bernardo-Bricker, W. Rogge, Environ. Sci. Technol. 40 (2006) 7803–7810.
[7] B. Van Drooge, P.P. Ballesta, Environ. Sci. Technol. 43 (2009) 7310–7316.
[8] J. Yin, R.M. Harrison, Q. Chen, A. Rutter, J. Schauer, Atmos. Environ. 44 (2010) 841–851.
[9] A. Dvorská, K. Komprdová, G. Lammel, J. Klánová, H. Plachá, Atmos. Environ. 46 (2012) 147–154.
[10] E. Galerneau, Atmos. Environ. 42 (2008) 8139–8149.
[11] S.D. Shah, T.A. Ogunyoku, J.W. Miller, D.R. Cocker III, Environ. Sci. Technol. 39 (2005) 5276–5284.
[12] G.C. Lough, C.G. Christensen, J.J. Schauer, J. Tortorelli, E. Mani, D.R. Lawson, N.N. Clark, P.A. Gabele, J. Air Waste Manage. Assoc. 57 (2007) 1190–1199.
[13] I. El Haddad, N. Marchand, J. Dron, B. Temime-Roussel, E. Quivet, H. Wortham, J.L. Jaffrezo, C. Baduel, D. Voisin, J.L. Besombes, G. Gille, Atmos. Environ. 43 (2009) 6190–6198.
[14] J. Orasche, J. Schnelle-Kreis, C. Schön, H. Ruppert, H. Hartmann, J.M. Arteaga-Salas, R. Zimmermann, Energy Fuels 27 (2013) 1482–1491.
[15] A. Felinger, M.C. Pietrogrande, Anal. Chem. 73 (2001) 618A–622A.
[16] M.C. Pietrogrande, M.G. Zampolli, F. Dondi, C. Szopa, R. Sternberg, A. Buch, F. Raulin, J. Chromatogr. A 1071 (2005) 255–261.
[17] M.C. Pietrogrande, M.G. Zampolli, F. Dondi, Anal. Chem. 78 (2006) 2576–2592.
[18] M.C. Pietrogrande, M. Mercuriali, L. Pasti, Anal. Chim. Acta 594 (2007) 128–138.
[19] M.C. Pietrogrande, M. Mercuriali, D. Bacco, Air Pollution XVI, in: C.A. Brebbia, Longhust J.W.S (Eds.), WITPress, Southampton (UK), 2008, pp. 335–343.
[20] M.C. Pietrogrande, M. Mercuriali, L. Pasti, F. Dondi, Analyst 134 (2009) 671–680.
[21] M.C. Pietrogrande, M. Mercuriali, M.G. Perrone, L. Ferrero, G. Sangiorgi, E. Bolzacchini, Environ. Sci. Technol. 44 (2010) 4232–4240.
[22] M.G. Perrone, L. Ferrero, B.R. Larsen, G. Sangiorgi, G. De Gennaro, G. Udisti, R. Zangrando, A. Gambaro, E. Bolzacchini, Sci. Total Environ. 414 (2012) 343–355.
[23] M.G. Perrone, M. Gualtieri, V. Consonni, L. Ferrero, G. Sangiorgi, E. Longhin, D. Ballabio, E. Bolzacchini, M. Camatini, Environ. Pollut. 176 (2013) 215–227.
[24] C.A. Belis, J. Cancelinha, M. Duane, V. Forcina, V. Pedroni, R. Passarella, G. Tanet, K. Dous, A. Piazzalunga, E. Bolzacchini, G. Sangiorgi, M.G. Perrone, L. Ferrero, P. Fermo, B.R. Larsen, Atmos. Environ. 45 (2011) 7266–7275.
[25] A. Piazzalunga, C. Belis, V. Bernardoni, O. Cazzuli, P. Fermo, G. Valli, R. Vecchi, Atmos. Environ. 45 (2011) 6642–6649.
[26] B.R. Larsen, S. Gilardoni, K. Stenstrom, J. Niedzialek, J. Jimenez, C.A. Belis, Atmos. Environ. 50 (2012) 203–213.
[27] V. Gianelle, C. Colombi, S. Caserini, S. Ozgen, S. Galante, A. Marongiu, G. Lanzani, Atmos. Pollut. Res. 2013, doi: 10.5094/APR.2013.028.
[28] C. Colombi, V. Gianelle, C.A Belis, B.R. Larsen, Chem. Eng. Trans. 22 (2010) 233–238.
[29] R.J. Delfino, C. Sioutas, S. Malik, Environ. Health Perspect. 113 (2005) 934–946.
[30] K. Saarnio, M. Sillanpa, R. Hillamo, E. Sandell, A.S. Pennanen, R.O. Salonen, Atmos. Environ. 42 (2008) 9087–9097.
[31] G. Vinyals, L. Bouso, M.C. Chalbot, I.G. Kavouras, R.O. Salonen, Sci. Total Environ. 374 (2007) 297–310.
[32] X.L. Zhang, S. Tao, W.X. Liu, Y. Yang, Q. Zuo, S.Z. Liu, Environ. Sci. Technol. 39 (2005) 9109–9114.
[33] J. Oda, S. Nomura, A. Yasuhara, T. Shibamoto, Atmos. Environ. 35 (2001) 4819–4827.